(Abstract submitted to the 35th IWWWFB, Seoul, Korea, 2020)

Non-linear hybrid model for forced heave of a shallowly submerged cylinder.

Guy McCauley[a]*, Hugh Wolgamot[a], Scott Draper[a] and Jana Orszaghova[a].
[a]Oceans Graduate School, the University of Western Australia, Perth, WA, Australia.
*Email: *guy.mccauley@research.uwa.edu.au*

1 Introduction

Wave interaction with shallowly submerged structures where the wave amplitude is of the same order of magnitude as the submergence is often a difficult problem to model numerically due to wave breaking, the formation of bores and other non-linearities. Linear hydrodynamic models perform poorly due to these effects. This work aims to develop a time domain hybrid numerical model for the forced heave of a shallowly submerged vertical axis cylinder, using linear potential flow in the region around the cylinder, matched to the non-linear shallow water equations for the region above the cylinder. This work is motivated by the Carnegie Clean Energy CETO wave energy device, a thin vertical axis cylinder ≈25m in diameter which sits 2-3m submerged below the free surface. For surface-piercing devices, parametric studies with linear hydrodynamic models are a key tool; for shallowly submerged devices linear theory may be inadequate due to the effects described above. It is of interest to create computationally efficient models using simplified non-linear equations, that may predict the bulk flow properties adequately for parametric design studies.

Previous work by the authors examined the performance of a hybrid potential flow - shallow water equations model for diffraction by a shallowly submerged step in 2D (McCauley et al., 2019). This model showed promise when comparing to simulations conducted in CFD. The matching scheme used in this model followed from Grue (1992), who matched potential flow to the Boussinesq equations in the shallow water region. The matching utilised an analytical form for a time-dependent source term at the boundary, the strength of which depends on the flow rate at the edge of the step. This matching method does not extend well to the 3D problem where a simple analytical form is not readily available, hence a new matching method has been used in the current work, where the surface elevation at the boundary in the potential flow domain is calculated using an impulse response function based on a pre-computed frequency domain solution to the exterior problem. Comparison of the hybrid model to experimental data will be shown.

2 Hybrid model matching scheme

Figure 1 defines the cylindrical coordinate system (r, θ, z). The fluid is divided into three regions, the core regions above and below the cylinder and an exterior region. The radius of the cylinder is a, the water depth h, the distance from the free surface to the top of the cylinder s and the clearance between the seafloor and the bottom of the cylinder is c. The flow in the exterior and lower core regions is modelled using the potential flow eigenfunction expansion method, following Siddorn & Eatock Taylor (2008), while the flow in the shallow water region is modelled using the non-linear shallow water equations, implemented using the finite volume method. In the linear exterior domain we decompose the potential into a component due to the heave oscillations of a surface piercing cylinder and a component due to the flow at the boundary between the exterior and top core region. Since the flow in the top core region is assumed to be shallow, i.e. $ks \ll 1$ (where k is the wavenumber), we approximate the flow at the boundary by a radially oscillating solid boundary, or "piston", where the velocity normal to the piston surface at $r = a$ is constant over $-s \leq z \leq 0$. Figure 2 shows the solution decomposition in the exterior region, where the total surface elevation at the boundary, η_E, is composed of η_{SP} due to the oscillating surface piercing cylinder and η_{PE} due to the oscillating solid piston boundary.

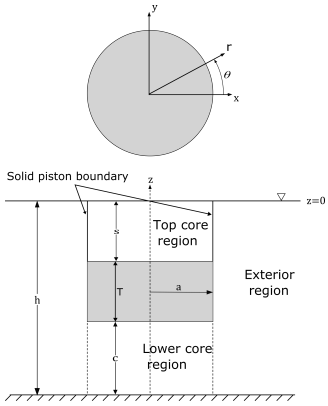

Figure 1: Definition sketch.

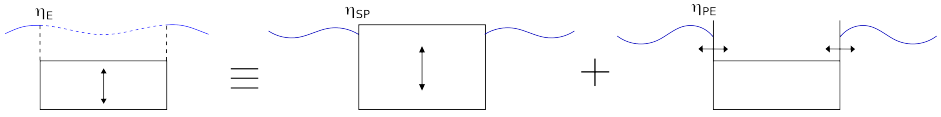

Figure 2: Solution decomposition in exterior region.

The general time marching scheme at the matching boundary for this forced motion problem is as follows:

1. The total surface elevation η_E is calculated at the current time step using η_{PE} from the previous step (zero in the first time step) and η_{SP} evaluated at the current time. This is used to force the shallow water solver.
2. The velocity at the top core boundary from the shallow water solver is used to calculate the surface elevation η_{PE} using the piston model impulse response function.
3. Steps 1 and 2 are repeated until the final time is reached.

3 Potential flow model

The potential flow model used for the surface piercing cylinder oscillating in heave follows Siddorn & Eatock Taylor (2008) and will not be described in full here. The angle invariant potential for each Fourier mode f is denoted χ_f and t is the time. The piston cylinder model uses the same method, modified by the additional boundary condition at $r = a$, $-s < z < 0$ and with zero normal velocity on the cylinder surface in the lower core region. The velocity potential in the exterior region is:

$$\chi_f^E(r,z) = \sum_{m=0}^{\infty} Z_m(z) A_{fm} \frac{P_{fm}(k_m r)}{P_{fm}(k_m a)}. \tag{1}$$

The functions P_{fm} are defined as

$$P_{fm}(k_m r) = \begin{cases} H_f^{(2)}(k_0 r) & m = 0 \\ K_f(\mathrm{i}k_m r) & m = 1, 2, ... \end{cases}, \tag{2}$$

where $H_f^{(2)} = J_f - \mathrm{i}Y_f$ and K_f are Bessel functions in the standard notation. The remaining boundary condition on the cylinder surface can be satisfied by choice of coefficients A_{fm}. The exterior region velocity potential depth dependence is described by the function $Z_m(z)$:

$$Z_m(z) = (N_m^E)^{-1/2} \cosh(k_m(z+h)). \tag{3}$$

The "piston" surface is assumed to extend vertically from $z = -s$ to the free surface at $r = a$. The radial velocity of the piston is assumed to be constant for all θ, the boundary condition on the piston surface is:

$$\left.\frac{\partial \chi_f^E}{\partial r}\right|_{r=a, -s \le z \le 0} = u_r. \tag{4}$$

The velocity potentials in the exterior and lower core are matched by integrating over the depth as in Siddorn & Eatock Taylor (2008) equation (18), giving the condition:

$$\alpha_{fn} = \sum_{m=0}^{\infty} A_{fm} C_{nm}, \tag{5}$$

where C_{nm} are coupling coefficients and α_{fn} are the lower core potential coefficients, see Siddorn & Eatock Taylor (2008). On the piston surface, we use boundary condition (4) to define coefficients D_m:

$$\begin{aligned} \frac{1}{h}\int_{-s}^{0} \left.\frac{\partial \chi_f^E}{\partial r}\right|_{r=a} Z_m(z)\mathrm{d}z &= \frac{1}{h}\int_{-s}^{0} u_r Z_m(z)\mathrm{d}z \\ &= \frac{u_r (N_m^E)^{1/2}}{k_m h}\left(\sinh(k_m h) - \sinh(k_m(h-s))\right) \\ &= u_r D_m. \end{aligned} \tag{6}$$

Including the integrals over $-h \le z \le -s$, see McCauley et al. (2018) equation (21), gives the key equation:

$$\sum_{n=0}^{\infty} \alpha_{fn} S_{fn} C_{nm} + u_r D_m = A_{fm} \frac{P'_{fm}(k_m a)}{P_{fm}(k_m a)}, \tag{7}$$

coefficients S_{fn} are defined in Siddorn & Eatock Taylor (2008). Equations (5) and (7) may be written as matrix equations and solved for the coefficients A_{fm} and α_{fn} (for the external and lower core regions, respectively). This completes the oscillating piston solution.

4 Surface elevation impulse response functions

The complex amplitude of the surface elevation at $r = a$ for a single heaving surface piercing cylinder is given by:

$$\hat{\eta}_{SP} = -\frac{\mathrm{i}\omega}{g} \sum_{m=0}^{\infty} Z_m(0) A_{0m}. \tag{8}$$

Noting that the exterior potential coefficients are given by $A_{0m} = D_m \mathbf{u}$ we can write

$$\hat{\eta}_{SP} = -\frac{\mathrm{i}\omega}{g} \sum_{m=0}^{\infty} Z_m(0) D_m \mathbf{u}. \tag{9}$$

Only considering heave motion we take $\mathbf{u} = \hat{u}_h[0, 0, 1, 0, 0, 0]^T$ where $\hat{u}_h$ is the complex heave velocity. Then we may write $\hat{\eta}_{SP} = H(\omega)\hat{u}_h$, where we have defined the frequency transfer function $H(\omega) = -\frac{\mathrm{i}\omega}{g} \sum_{m=0}^{\infty} Z_m(0) D_m [0, 0, 1, 0, 0, 0]^T$. Assuming that the impulse response function (IRF), $h(t)$, is real and causal, then $H(\omega)$ is Hermitian implying the real part is an even function and the imaginary part is an odd function. It follows that the IRF, which is the inverse Fourier transform of the transfer function, can be written as:

$$h(t) = \frac{1}{2\pi} \int_{-\infty}^{\infty} H(\omega) e^{\mathrm{i}\omega t} \mathrm{d}\omega = \frac{2}{\pi} \int_{0}^{\infty} \mathrm{Re}\{H(\omega)\} \cos(\omega t) \mathrm{d}\omega. \tag{10}$$

Thus only the real part of the transfer function is required in computation of the IRF. The real part approaches zero for high frequency faster than the imaginary part, reducing numerical error due to truncating the above integral at a cut off frequency. The time domain surface elevation at the cylinder edge can then be calculated by the convolution integral of the IRF with the time series of body heave velocity:

$$\eta_{SP}(t) = \int_{-\infty}^{t} u_h(\tau) h(t - \tau) \mathrm{d}\tau. \tag{11}$$

In practice the convolution integral above is approximated using the Prony method. The piston surface elevation impulse response function is calculated in a similar way, however it requires special attention as neither the real or imaginary parts of the transfer function for surface elevation at the piston edge approach zero quickly at high frequency. An infinite frequency approximation for this transfer function has been derived, which allows a closed form integral of the approximate transfer function to be used above a high frequency cut-off in evaluation of (10).

5 Shallow water equations

The shallow water equations are used to model the flow in the top core region. As we are considering only heave motion the problem is axi-symmetric and we may use the shallow water equations for cylindrical symmetry, given by Toro (2001) p246 equation (13.6). These are solved using a MUSCL Hancock scheme, HLL Riemann solver and splitting scheme for the source terms. The shallow water solver has been verified for small amplitude cases using the solution of Lamb (1993) (see p275) for canals of varying cross section.

6 Results

The hybrid model is compared to experimental data from a testing campaign at the COAST laboratory, University of Plymouth, UK in 2018. In the basin tests motions of a submerged buoyant cylinder were imposed using a taut 3-cable arrangement. Forces in the cables and surface elevation at $r = 0$ were measured. Sinusoidal cable motions were imposed, but due to the cable geometry the resulting heave motion profiles differed slightly from sinusoidal. These tests were undertaken by UWA in collaboration with Carnegie Clean Energy. The experimental data is compared to the hybrid model as well as a linear potential flow model for a submerged cylinder as described in McCauley et al. (2018). For the linear model, impulse response functions for the surface elevation and force are used to generate the time domain result given input heave body motion from the experiments.

Figure 3 shows the surface elevation at the centre of the cylinder (top row), surface elevation in the exterior field at $r/a = 3.1$ (second row), cylinder heave displacement denoted by ζ (third row) and heave hydrodynamic force (fourth row). In this test case $ka = 0.35$ and $A/s = 0.33$ where A is the heave amplitude. The vertical magenta line indicates the expected arrival time of reflections (first harmonic) from the tank side-walls. The surface elevation in the exterior field has been low pass filtered with the cut off at six times the fundamental frequency. It can be seen that the hybrid model performs significantly better than the linear model in predicting the surface elevation and (particularly) the force in this case. Higher harmonics in the force

do not appear to be captured well, but the agreement is very good otherwise. Figure 4 shows the same plots at $ka = 0.42$, $A/s = 0.34$. The hybrid model performs well at lower frequencies, however above $ka = 0.6$ the hybrid model performs rather poorly when comparing the hydrodynamic force to experiments. Further results at other frequencies and amplitudes will be shown at the workshop.

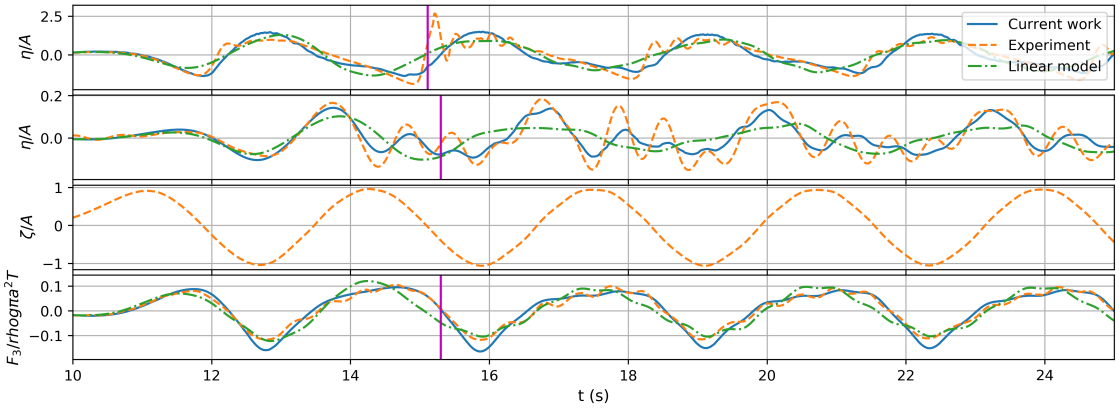

Figure 3: Surface elevation at the cylinder centre and at $r/a = 3.1$, heave displacement and vertical hydrodynamic force. $ka = 0.35$, $A/s = 0.33$, $s/a = 0.16$, $h/a = 2.4$, $T/a = 0.4$.

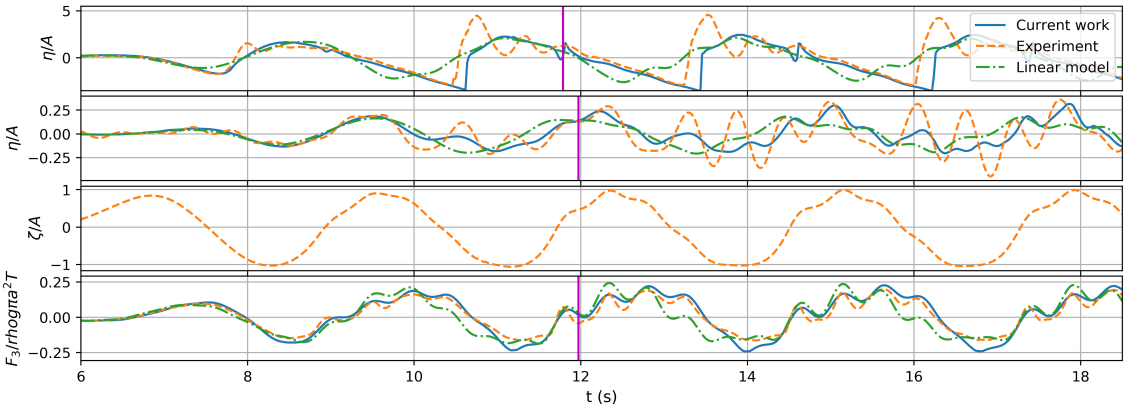

Figure 4: Surface elevation at the cylinder centre and at $r/a = 3.1$, heave displacement and vertical hydrodynamic force. $ka = 0.42$, $A/s = 0.34$, $s/a = 0.16$, $h/a = 2.4$, $T/a = 0.4$.

Acknowledgments

The authors would like to acknowledge Professor Rodney Eatock Taylor for his many helpful suggestions concerning this work. GM, HW and SD acknowledge the support of the Lloyds Register Foundation. HW also acknowledges financial support from Shell Australia. This work forms part of the activities conducted within the ARC Linkage Project 150100598. The laboratory tests in the COAST laboratory at the University of Plymouth, UK were supported by MaRINET2 funding.

References

Grue, J 1992, 'Nonlinear water waves at a submerged obstacle or bottom topography', *J. Fluid. Mech.*, vol. 244, pp. 455–476.

Lamb, H 1993, *Hydrodynamics*, Cambridge University Press.

McCauley, G, Wolgamot, H, Orszaghova, J & Draper, S 2018, 'Linear hydrodynamic modelling of arrays of submerged oscillating cylinders', *Applied Ocean Research*, vol. 81, pp. 1–14.

McCauley, G et al. 2019, 'Wave interaction with a shallowly submerged step', '34th IWWWFB', Newcastle, Australia.

Siddorn, P & Eatock Taylor, R 2008, 'Diffraction and independent radiation by an array of floating cylinders', *Ocean Eng.*, vol. 35, no. 13, pp. 1289–1303.

Toro, EF 2001, *Shock-capturing methods for free-surface shallow flows*, Wiley and Sons Ltd.